

Immuno-Polymeric Nanoparticles by Diels–Alder Chemistry**

Meng Shi, Jordan H. Wosnick, Karyn Ho, Armand Keating, and Molly S. Shoichet*

Immuno-nanoparticles hold great promise for targeted delivery of drugs, therapeutics, and diagnostics as numerous possible target receptors have been identified on the surface of cells in pathological conditions.^[1–4] Under in vivo conditions, immuno-nanoparticles can deliver these agents to specific sites by both passive targeting, where a hydrophilic polymer outer layer such as polyethylene glycol (PEG) leads to longer circulation in the blood stream,^[1,3–5] and active targeting mechanisms, where the “passive” nanoparticles have antibody molecules or fragments covalently coupled to their surface to achieve localized delivery to target cells that express the corresponding antigen receptors.^[1,3,4] The design of immuno-polymeric nanoparticles requires not only the creation of well-defined structures, but also the optimization of antibody conjugation chemistry.^[3,4,6–13] Here we report the design of a novel polymeric nanoparticle system using new biodegradable graft copolymers of poly(2-methyl-2-carboxy-trimethylene carbonate-co-D,L-lactide)-*graft*-poly(ethylene glycol)-furan (poly(TMCC-co-LA)-*g*-PEG-furan; Scheme 1) that self-assemble into micellar nanoparticles in aqueous solution and provide reactive functional groups for coupling of antibodies through Diels–Alder reactions.

Polymeric amphiphiles^[14–22] self-assemble upon contact with aqueous environments; the hydrophobic regions of the copolymers spontaneously aggregate together to minimize contact with the aqueous environment while the hydrophilic segments are exposed to the aqueous environment and form the outer corona. The inner hydrophobic domain, surrounded by a hydrophilic outer shell, has been used to encapsulate

hydrophobic small molecules primarily. The interest in micellar self-assembling polymeric nanoparticles as delivery vehicles is growing because they can both stabilize hydrophobic molecules at high drug loading and have their composition tuned to allow functionalization.^[3,14–22] Although various polymeric micellar systems have been developed as delivery vehicles, only a few cases have been designed to incorporate antibodies for immunotargeting.^[3]

To couple antibodies or antigen-binding fragments, mild reaction conditions are required to achieve high efficiency without significant loss of binding activity. While a number of techniques for antibody conjugation have been established,^[3,6–13] these conventional methods often require either activation^[6,8] or coupling reagents,^[10] thereby increasing the complexity of the reaction protocol and the possibility of side reactions. Moreover, the highly reactive nature^[6–8,12,13] and instability^[11] of the functional groups limit the efficiency of these methods.

Diels–Alder reactions, which involve a highly selective [4+2] cycloaddition reaction between a diene and a dienophile,^[23–25] provide a means to overcome the limitations associated with coupling chemically sensitive antibody molecules, particularly in aqueous environments where both the rate and stereoselectivity of Diels–Alder reactions are dramatically increased.^[24,25] The great potential of Diels–Alder reactions in biotechnology applications has been recognized,^[26–30] and here we demonstrate its applicability to conjugate antibodies to nanoparticles for targeted delivery. This simple, one-step reaction without by-products does not require initiators, catalysts, or coupling reagents, is highly efficient and selective under mild conditions, and results in stable products. Our nanoparticles were designed with furan groups (diene) on the outer PEG corona which are accessible for reaction with antibodies functionalized with maleimide (dienophile) groups in aqueous solution (Scheme 2). With a view toward targeted delivery in breast cancer, we demonstrate the synthesis of furan-functionalized micellar nanoparticles derivatized with maleimide-modified anti-HER2 (a therapeutic antibody used to treat breast cancer) through Diels–Alder reactions and the specific and efficient binding with breast cancer HER2-over-expressing cell lines in vitro. This nanoparticle system provides a novel means for the delivery of combination immunotherapy/chemotherapy to more effectively treat certain malignancies.

The copolymer, poly(TMCC-co-LA)-*g*-PEG-furan, was designed specifically for the creation of immuno-nanoparticles by combining strategies of polymeric self-assembly and Diels–Alder reactions of bioconjugation in one process. The copolymer is biodegradable and biocompatible for in vivo applications; amphiphilic with the ability to self-assemble into ordered structures; and capable of undergoing Diels–Alder reactions because of the presence of furan groups at the PEG

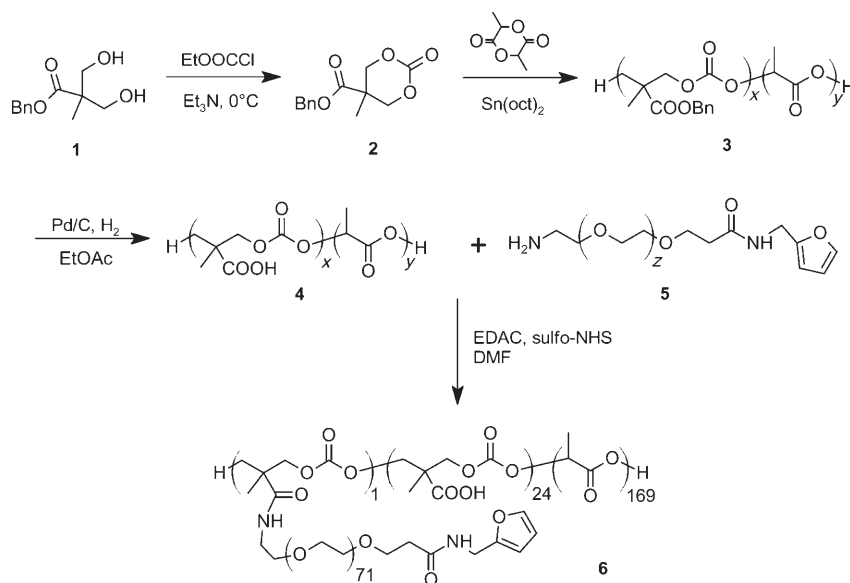
[*] M. Shi, Dr. J. H. Wosnick, K. Ho, Dr. M. S. Shoichet
Department of Chemical Engineering and Applied Chemistry
Department of Chemistry
Institute for Biomaterials and Biomedical Engineering
Terrence Donnelly Centre for Cellular and Biomolecular Research
University of Toronto
160 College Street, Toronto, ON M5S3E1 (Canada)
Fax: (+1) 416-978-4317
E-mail: molly@chem-eng.utoronto.ca
Homepage: <http://www.ecf.utoronto.ca/~molly>
Dr. A. Keating
Cell Therapy Program
Princess Margaret Hospital/Ontario Cancer Institute
University Health Network, 620 University Avenue
Toronto, ON (Canada)

[**] We thank Yumin Yuan for initial studies on the poly(TMCC-co-LA) synthesis, Professor Mitchell Winnik for helpful discussions, and Dr. Neil Coombs for TEM imaging. We are grateful to the Natural Sciences and Engineering Research Council and the Canadian Institutes for Health Research for funding through the Collaborative Health Research Program.

Supporting information (including characterization data) for this article is available on the WWW under <http://www.angewandte.org> or from the author.

termini. Scheme 1 shows the synthesis of the amphiphilic copolymer. The resulting amphiphilic copolymer of 19.2 kg mol^{-1} contains a hydrophobic backbone of

terminal furan groups are easily accessible to maleimide-functionalized molecules in the aqueous solution, thus enabling cycloaddition at the PEG termini of self-assembled nanoparticles (Scheme 2).

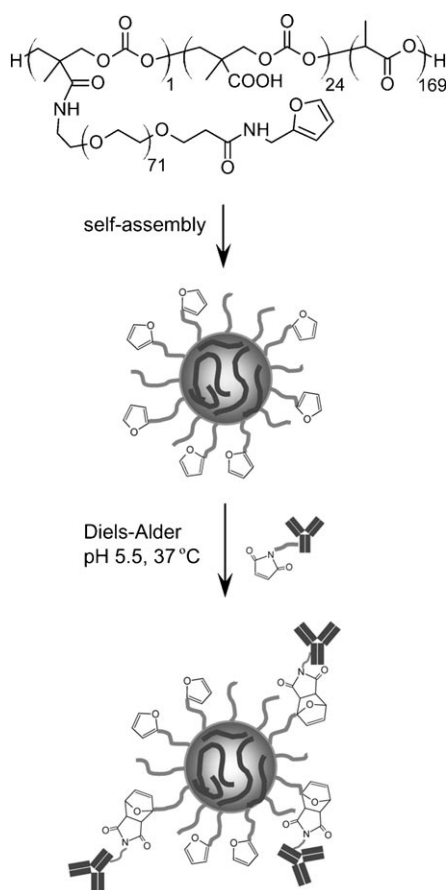


Scheme 1. Synthesis of poly(TMCC-*co*-LA)-*g*-PEG-furan amphiphilic graft copolymer: The copolymer backbone of poly(TMCC-*co*-LA) (4) was synthesized by ring-opening polymerization of the cyclic carbonate monomer 2 (benzyl-protected TMCC), and D,L-lactide (LA) to yield various copolymer compositions; the random copolymer with 13 mol% TMCC and 87 mol% LA are described in detail herein. Poly(TMCC-*co*-LA) was then modified with a bifunctional furan-poly(ethylene glycol)-amine (furan-PEG-NH₂) (5) by coupling amine-terminated PEG to the pendant carboxylic acid groups on the backbone polymer. The resulting amphiphilic, 19.2 kg mol^{-1} copolymer contains a hydrophobic backbone of poly(TMCC-*co*-LA) and an average of one hydrophilic PEG chain grafted per backbone. (see Section S1 and Table S1 in the Supporting Information for polymer characterization). Bn = benzyl.

poly(TMCC-*co*-LA) and hydrophilic grafts of PEG with furan groups located at the PEG termini. The amphiphilic copolymer was dissolved in a mixture of dimethylformamide (DMF) and borate buffer and dialyzed against distilled water to drive self-assembly. Scheme 2 shows a schematic representation of the self-assembly of micellar nanoparticles. The hydrophobic segments of the poly(TMCC-*co*-LA) backbone form the dense inner core while the hydrophilic PEG chains orient toward the aqueous solution to form the outer corona. Well-formed spherical nanoparticles were observed by transmission electron microscopy (TEM; see Figure S1 in the Supporting Information) and have a hydrodynamic diameter of 84 nm measured by dynamic light scattering. The formation of hydrophobic microdomains in the micellar nanoparticles was confirmed by fluorescence measurements using pyrene. According to this method, the apparent critical aggregation concentration (CAC_{app}) of the copolymer was determined to be approximately $3 \mu\text{g mL}^{-1}$ (see Figure S2 in the Supporting Information). In this system, the furan-maleimide Diels-Alder reaction was designed to occur at the interface between the PEG corona of the nanoparticles and the aqueous phase in which the antibodies are dissolved. After the amphiphilic copolymer self-assembles into micellar nanoparticles, the hydrophilic segments orient outward to the water phase. The

To demonstrate the utility of poly(TMCC-*co*-LA)-*g*-PEG micellar nanoparticles as targeting vehicles, we constructed immuno-nanoparticles by derivatizing preformed micellar nanoparticles with herceptin (anti-HER2), a therapeutic monoclonal antibody used to treat breast cancer. Herceptin is known to bind to human epidermal growth factor receptor-2 (HER2), which is over-expressed on 20–30% of breast and ovarian cancer cell surfaces,^[31] thereby providing a basis for selective immunotargeting in our system.

To couple herceptin antibodies (anti-HER2) to the micellar nanoparticles by Diels-Alder reactions, an established site-specific modification of the carbohydrate chains within the Fc region of anti-HER2 was achieved. This enabled the introduction of maleimide (Mal) groups while preserving the intact Fab fragment for antigen binding and minimizing the loss of the bioactivity^[32,33] (see Figure S3 in the Supporting Information on modification of antibodies at the Fc region). The average number of maleimide groups introduced per antibody was approximately two. By using flow cytometry to compare the binding capacity of maleimide-modified anti-HER2 (anti-HER2-Mal) versus anti-HER2 to HER2-over-expressing SKBR3 breast cancer cells, it was confirmed that the modification of anti-HER2 with maleimide did not affect its binding capacity (see Figure S4 in the Supporting Information). Immuno-nanoparticles were prepared by incubating



Scheme 2. Schematic representation of the self-assembly of micellar nanoparticles from poly(TMCC-co-LA)-g-PEG-furan and Diels-Alder reactions between the nanoparticles and maleimide-modified antibodies: the hydrophobic segments of poly(TMCC-co-LA) form the inner core and the hydrophilic PEG chains orient toward the aqueous solution to form the outer corona. Furan groups are located at PEG termini which are easily accessible to maleimide-modified antibodies for Diels-Alder reactions.

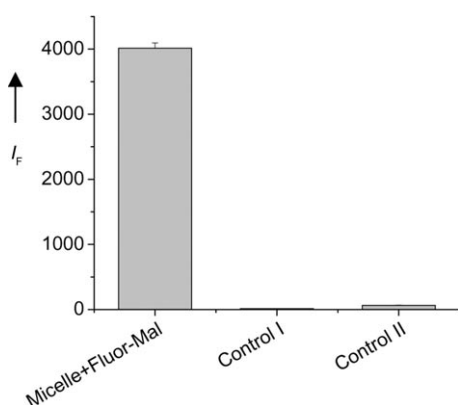


Figure 1. Maleimide-containing Alexa Fluor 488 C₅-Maleimide (Fluor-Mal) coupled to furan groups of self-assembled micellar nanoparticles by Diels-Alder reactions. Control I: Maleimide groups on Fluor-Mal fluorescent probes were quenched by incubating with excess cysteine prior to reaction with furan-functionalized nanoparticles. Control II: Maleimide groups on Fluor-Mal fluorescent probes were quenched by incubating with excess furfurylamine prior to reaction with furan-functionalized nanoparticles (shown are the mean values of three measurements \pm standard deviation).

anti-HER2-Mal with nanoparticles in MES buffer at pH 5.5 and 37 °C (without any additional reagents). When the nanoparticle/anti-HER2-Mal feed mass ratio was kept constant (for example at 100:1), both the anti-HER2 density on the immuno-nanoparticles and the coupling efficiency (expressed as the percentage of the initial feed antibody bound to the micellar nanoparticles) increased as a function of reaction time (Figure 2a). Almost 100 % of the initial anti-HER2-Mal added was coupled within six hours of incubation, thus resulting in an antibody density of 64 pmol mg⁻¹ nanoparticle (approximated at 5 antibodies per nanoparticle; see Section S4 in the Supporting Information). To better understand the parameters that influence the yield of this Diels-Alder reaction, the reaction time was fixed at 2 h and the initial nanoparticle/anti-HER2-Mal mass ratio was increased. As shown in Figure 2b, the coupling efficiency increased as the nanoparticle/anti-HER2-Mal mass ratio increased; however, as might be expected, the anti-HER2 density on the immuno-nanoparticle decreased. By using Diels-Alder reac-

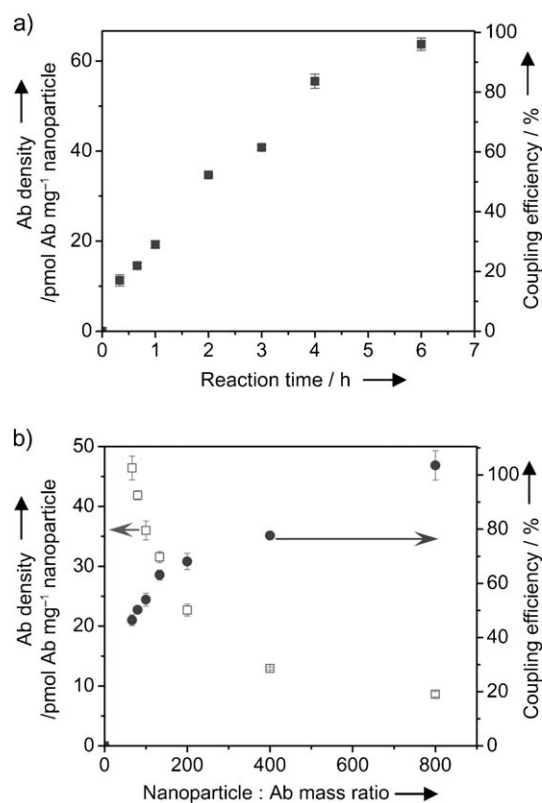


Figure 2. Immuno-nanoparticles prepared by Diels-Alder reactions. a) Representative time-dependence of the coupling of anti-HER2-Mal to nanoparticles. Reactions were carried out in pH 5.5 MES buffer at 37 °C. The nanoparticle/anti-HER2-Mal mass feed ratio was fixed at 100:1. Anti-HER2-Mal was labeled with a fluorescent dye (Alexa Fluor 430) for quantification. The coupling efficiency is expressed as the percentage of the initial feed antibody bound to the micellar nanoparticles. b) Representative nanoparticle/anti-HER2-Mal feed ratio dependence of coupling of anti-HER2-Mal to nanoparticles. Reaction time was fixed at 2 h. (see Section S4 in the Supporting Information: the antibody density was converted into the average number of antibody molecules per nanoparticle by estimating the aggregation number of the micellar nanoparticles). Ab = antibody.

tions, either prolonged reaction times or high nanoparticle/anti-HER2-Mal feed ratios can be used to achieve maximum coupling efficiency. The large excess of accessible nanoparticle furan groups relative to maleimide-modified antibodies may account for the rapid reaction and the high coupling efficiency achieved. To better understand the coupling capacity of the furan-functionalized nanoparticles in the Diels–Alder reaction, anti-HER2-coupled micellar nanoparticles were further modified with maleimide-containing fluorescent probes. It was found that after coupling of the antibody, the immuno-nanoparticle coupled a similar amount of fluorescent probe as the unmodified (plain) nanoparticles. When we compared the number of furan sites occupied by the antibodies ($11\text{--}64\text{ pmol mg}^{-1}$ nanoparticle) with the total number of accessible furan groups for the Diels–Alder reaction (3.6 nmol mg^{-1} nanoparticle, as determined with small fluorescent probe molecules), we found that the bound antibodies occupied only 1–2% of the accessible furan groups. This finding suggests that, even after coupling of the antibody, the majority of furan groups are available for further modification, thus allowing the nanoparticles to serve multiple functions by sequential Diels–Alder reactions, for example, of targeting ligands, imaging agents, and/or drug molecules.

Importantly the hydrodynamic diameter of the immuno-nanoparticles, $86.6 \pm 3.4\text{ nm}$ was similar to that of unmodified (plain) nanoparticles, $84.3 \pm 2.6\text{ nm}$, (see Figure S5 in the Supporting Information), which suggests that neither aggregation nor cross-linking occurred during the antibody-coupling procedure.

To demonstrate the capability of anti-HER2 immuno-nanoparticles to bind specifically with HER2-over-expressing cells, the immuno-nanoparticles were incubated with the following cell lines: SKBR3 (HER2-over-expressing), MCF7 (HER2-low-expressing), and MDA-

MB-468 (HER2 negative). Flow cytometry was employed to measure the cell-associated fluorescence above background. As shown in Figure 3a,b, the anti-HER2 immuno-nanoparticles showed fourfold higher binding activity with SKBR3 than the IgG1K immuno-nanoparticle control (IgG1K acts as a nonspecific antibody and shows little binding with SKBR3). The binding of the immuno-nanoparticles was much lower with low-HER2-expressing MCF7 cells than that observed with SKBR3 cells. No binding was observed for the HER2-negative MDA-MB-468 cells (Figure 3b). The binding of immuno-nanoparticles correlates with the HER2 expression levels in these cell lines, which is well-documented^[31] and was confirmed by incubation with herceptin under the same conditions and by subsequent labeling with an FITC-anti-

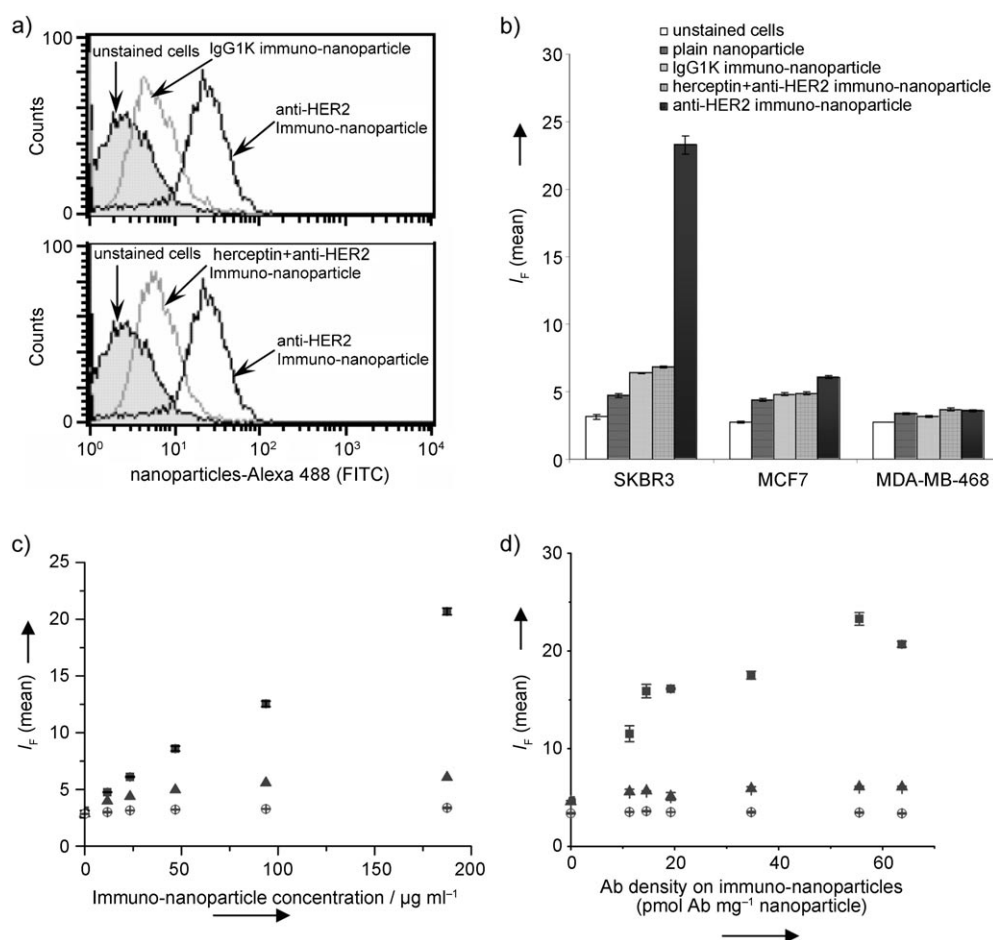


Figure 3. Anti-HER2 immuno-nanoparticles binding with HER2-over-expressing cells. a) Flow cytometry analysis of the specific binding of anti-HER2 immuno-nanoparticles with SKBR3 cells (HER2-over-expressing): Top: Comparison of the binding of anti-HER2 immuno-nanoparticles and nonspecific IgG1K immuno-nanoparticles. The antibody density on the anti-HER2 immuno-nanoparticles was 56 pmol mg^{-1} nanoparticle. IgG1K immuno-nanoparticles with the same antibody density were prepared under the same conditions as the anti-HER2 immuno-nanoparticles; bottom: Binding of anti-HER2 immuno-nanoparticles with SKBR3 cells presaturated with anti-HER2. b) Mean fluorescent intensity measured for immuno-nanoparticles binding with SKBR3 cells (HER2-over-expressing), MCF7 (HER2-low-expressing), and MDA-MB-468 (HER2-negative) cells, determined by flow cytometry. c) Representative dose-dependence for the binding of anti-HER2 immuno-nanoparticles with (■) SKBR3, (▲) MCF7, and (○) MDA-MB-468 cells. The antibody density was fixed at 64 pmol mg^{-1} nanoparticle. d) Representative dependence of the antibody density of the binding of anti-HER2 immuno-nanoparticles with SKBR3, MCF7, and MDA-MB-468 cells. The concentration of the immuno-nanoparticles was fixed at $187.5\text{ }\mu\text{g mL}^{-1}$ (shown are the mean values of three measurements \pm standard deviation).

human antibody (see Figure S6 in the Supporting Information). As further confirmation of the specificity of the interaction of the immuno-nanoparticles with cells, presaturation of HER2 antigens on SKBR3 cells with free herceptin was found to inhibit the binding of immuno-nanoparticles with SKBR3 cells by more than 70 % (Figure 3b). The binding capacity of the immuno-nanoparticles to SKBR3 cells increased with increased concentrations of immuno-nanoparticles (Figure 3c). A significantly lower, but similar observation was made with MCF7 cells, and there was no measurable dose-dependent effect of immuno-nanoparticle concentration on binding to HER2-negative MDA-MB-468 cells. The binding capacity of herceptin immuno-nanoparticles to SKBR3 cells increased as the density of herceptin per immuno-nanoparticle increased (Figure 3d); there was no effect of an increased herceptin density on binding to either MCF7 or MDA-MB-468 cell lines.

This proof-of-concept for cancer cell targeting with these immuno-nanoparticles has demonstrated the continued bioactivity, binding capacity, and specificity of the anti-HER2-coupled nanoparticles. The success that we have achieved can be attributed to the herceptin antibody being specifically modified with maleimide groups in its Fc fragment prior to nanoparticle coupling to avoid altering the binding characteristics of the antibody. Moreover, the mild aqueous conditions required for Diels–Alder cycloadditions of the antibodies to the nanoparticles avoids both long reaction times and the use of coupling or potentially denaturing reagents, thereby preserving the selectivity and efficient binding capability of the immobilized antibodies. Importantly, the antibodies are coupled to the terminal groups of the PEG corona which are easily accessible to antigen receptors on the cell surfaces.

In conclusion, we have synthesized new biodegradable, amphiphilic, furan-functionalized copolymers that self-assemble in aqueous conditions to form micellar nanoparticles. By designing the nanoparticles with furan functional groups at the termini of the PEG corona, anti-HER2 breast cancer antibodies, modified with maleimide functional groups in their Fc region, were covalently bound to the nanoparticles by Diels–Alder cycloadditions. Anti-HER2 immuno-nanoparticles specifically bound with HER2-over-expressing cells, thus demonstrating the capacity of this technique to create bioactive immuno-nanoparticles. The versatility of the nanoparticle system can be extended to create complex and multiple functional delivery vehicles by taking advantage of the Diels–Alder reaction to immobilize molecules appropriate for imaging, diagnostics, or the targeted delivery of therapeutic agents. Combining immunotherapy with locally delivered bioactive agents or chemotherapy is under investigation.

Experimental Section

2 (benzyl-protected TMCC): Compound **1** (12.7 g, 0.08 mol), derived by nucleophilic substitution of the sodium salt of 2,2-bis(hydroxymethyl)propionic acid with benzyl bromide, and ethyl chloroformate (19.1 g, 0.176 mol) were dissolved in THF (250 mL). The reaction solution was cooled in an ice bath under nitrogen (N_2). Triethylamine (19.4 g, 0.192 mol) was added dropwise to the rapidly stirring solution.

The reaction mixture was stirred in an ice bath under N_2 overnight, then filtered, and concentrated by rotary evaporation. The residue was recrystallized twice from ethyl acetate and dried in a vacuum oven overnight at RT to yield **2** as a white solid (13.5 g, 84 %).

3: Monomer **2** (2.5 g, 0.01 mol) was copolymerized with D,L-lactide (LA; 6.5 g, 0.045 mol) in a bulk melt in the presence of one drop of stannous 2-ethylhexanoate ($Sn(oct)_2$) at 120 °C for 24 h. The resulting product was then dissolved in chloroform and precipitated twice with hexane. After drying the product in a vacuum oven overnight at RT, the copolymer **3** was collected (6.8 g, 76 %).

4: Copolymer **3** (6.0 g) was dissolved in EtOAc and the benzyl protecting groups removed under hydrogen (H_2) in the presence of palladium on activated carbon (10 wt %) for 48 h at RT. The resulting polymer was then filtered and precipitated twice with hexane. After drying the product in a vacuum oven overnight at RT, the copolymer **4** was collected (4.4 g, 82 %).

6: Copolymer **4** (100 mg) was dissolved in DMF (5 mL) and MES buffer (0.5 mL; 10 mM, pH 5.5). *N*-ethyl-*N'*-(3-dimethylaminopropyl)carbodiimide hydrochloride (EDAC, 10 wt %) and *N*-hydroxysulfosuccinimide (sulfo-NHS, 10 wt %) were added. The reaction solution was incubated at RT for 30 min. The furan-PEG-NH₂ **5** (50 mg; see Section S1 in the Supporting Information for synthesis details) was dissolved in borate buffer (1 mL; 500 mM, pH 9.0). This solution was then slowly added to the activated copolymer **4** solution under stirring. The reaction mixture was incubated at RT for 24 h, after which the reaction solution was dialyzed against distilled water and then passed through a sepharose 4B column equilibrated with distilled water to remove any remaining PEG. The collected fractions containing particle suspensions were freeze-dried and copolymer **6** was collected as a white solid (75 mg, 50 %).

Nanoparticle preparation by the dialysis method: Poly(TMCC-co-LA)-g-PEG-furan **6** was dissolved in DMF/borate buffer (500 mM, pH 9.0) at a concentration of 10 mg mL⁻¹. The solution was dialyzed against distilled water using a dialysis membrane with a molecular-weight cut off (MWCO) of 12–14 kg mol⁻¹ at RT for 24 h (see Section S2 in the Supporting Information for detailed methods).

Immuno-nanoparticle preparation by Diels–Alder reactions: Nanoparticle solution (1 mL; 4.0 mg mL⁻¹ in distilled water) was added to a solution of the maleimide-modified antibody (1 mg mL⁻¹ in 100 mM MES buffer of pH 5.5). The reaction solution was incubated at 37 °C under gentle agitation for various time periods. The immuno-nanoparticles were purified by passing through a sephacryl S-300HR column in 10 mM phosphate-buffered saline (PBS) at pH 7.4 (see Sections S3 and S4 in the Supporting Information for detailed methods).

Immuno-nanoparticle binding with cells: The antibody-coupled immuno-nanoparticles were labeled with Alexa Fluor 488 C₅-Maleimide by the same Diels–Alder reaction as used for the flow cytometry analysis. 2×10^5 cells were suspended in 0.05 mL PBS buffer of pH 7.4 with 4 % fetal bovine serum (FBS) and then added to a solution of the immuno-nanoparticles (0.15 mL, various concentrations in 10 mM PBS, pH 7.4). After incubation of the mixture at 4 °C for 30 min, PBS buffer (1 mL) with 1 % FBS and 2 mM ethylenediamine tetraacetic acid (EDTA) was added to rinse the cells and the mixture was then centrifuged. The supernatant was removed. The harvested cells were resuspended in PBS buffer (0.5 mL) with 1 % FBS and 6 μ g mL⁻¹ propidium iodide and then analyzed by flow cytometry. The first 10^4 events were recorded for subsequent analysis of the gated live-cell population. For controls where HER2 receptors on the breast cancer cell lines were presaturated prior to interaction with immuno-nanoparticles, cells were incubated with excess free herceptin (10 μ g mL⁻¹) at 37 °C for 30 min prior to their incubation with the immuno-nanoparticles. (see

Sections S4 and S5 in the Supporting Information for detailed methods).

Received: March 7, 2007

Revised: May 28, 2007

Published online: July 12, 2007

Keywords: bioorganic chemistry · cycloaddition · drug delivery · micelles · self-assembly

- [1] T. M. Allen, *Nat. Rev. Cancer* **2002**, *2*, 750–763.
- [2] R. F. Service, *Science* **2005**, *310*, 1132–1134.
- [3] V. P. Torchilin, A. N. Lukyanov, Z. Gao, B. Papahadjopoulos-Sternberg, *Proc. Natl. Acad. Sci. USA* **2003**, *100*, 6039–6044.
- [4] V. P. Torchilin, *Nat. Rev. Drug Discovery* **2005**, *4*, 145–160.
- [5] S. M. Moghimi, A. C. Hunter, J. C. Murray, *Pharmacol. Rev.* **2001**, *53*, 283–318.
- [6] T. M. Allen, E. Brandeis, C. B. Hansen, G. Y. Kao, S. Zalipsky, *Biochim. Biophys. Acta* **1995**, *1237*, 99–108.
- [7] P. Benzinger, G. Martiny-Baron, P. Reusch, G. Siemeister, J. T. Kley, D. Marmé, C. Unger, U. Massing, *Biochim. Biophys. Acta Biomembr.* **2000**, *1466*, 71–78.
- [8] G. N. C. Chiu, M. B. Bally, L. D. Mayer, *Biochim. Biophys. Acta Biomembr.* **2003**, *1613*, 115–121.
- [9] J. A. Harding, C. M. Engbers, M. S. Newman, N. I. Goldstein, S. Zalipsky, *Biochim. Biophys. Acta Biomembr.* **1997**, *1327*, 181–192.
- [10] T. Mizoue, T. Horibe, K. Maruyama, T. Takizawa, M. Iwatsuru, K. Kono, H. Yanagie, F. Moriyasu, *Int. J. Pharm.* **2002**, *237*, 129–137.
- [11] V. P. Torchilin, T. S. Levchenko, A. N. Lukyanov, B. A. Khaw, A. L. Klivanov, R. Rammohan, G. P. Samokhin, K. R. Whiteman, *Biochim. Biophys. Acta Biomembr.* **2001**, *1511*, 397–411.
- [12] L. Nobs, F. Buchegger, R. Gurny, E. Allémann, *Bioconjugate Chem.* **2006**, *17*, 139–145.
- [13] R. Shukla, T. P. Thomas, J. L. Peters, A. M. Desai, J. Kukowska-Latallo, A. K. Patri, A. Kotlyar, J. R. Baker, Jr., *Bioconjugate Chem.* **2006**, *17*, 1109–1115.
- [14] G. Gaucher, M. H. Dufresne, V. P. Sant, N. Kang, D. Maysinger, J. C. Leroux, *J. Controlled Release* **2005**, *109*, 169–188.
- [15] E. S. Lee, K. Na, Y. H. Bae, *Nano Lett.* **2005**, *5*, 325–329.
- [16] N. Nasongkla, X. Shuai, H. Ai, B. D. Weinberg, J. Pink, D. A. Boothman, J. Gao, *Angew. Chem.* **2004**, *116*, 6483–6487; *Angew. Chem. Int. Ed.* **2004**, *43*, 6323–6327.
- [17] F. Zeng, H. Lee, C. Allen, *Bioconjugate Chem.* **2006**, *17*, 399–409.
- [18] V. Schmidt, C. Giacomelli, F. Lecolley, J. Lai-Kee-Him, A. R. Brisson, R. Borsali, *J. Am. Chem. Soc.* **2006**, *128*, 9010–9011.
- [19] S. Kwon, J. H. Park, H. Chung, I. C. Kwon, S. Y. Jeong, *Langmuir* **2003**, *19*, 10188–10193.
- [20] Y. Wang, S. Gao, W. H. Ye, H. S. Yoon, Y. Y. Yang, *Nat. Mater.* **2006**, *5*, 791–796.
- [21] R. Kumar, M. H. Chen, V. S. Parmar, L. A. Samuelson, J. Kumar, R. Nicolosi, S. Yoganathan, A. C. Watterson, *J. Am. Chem. Soc.* **2004**, *126*, 10640–10644.
- [22] N. Nishiyama, Y. Bae, K. Miyata, S. Fukushima, K. Kataoka, *Drug Discovery Today Technol.* **2005**, *2*, 21–26.
- [23] D. L. Boger, S. M. Weinreb, *Hetero Diels-Alder methodology in organic synthesis*, Academic Press, San Diego, **1987**.
- [24] S. Otto, J. B. F. N. Engberts, *Org. Biomol. Chem.* **2003**, *1*, 2809–2820.
- [25] D. C. Rideout, R. Breslow, *J. Am. Chem. Soc.* **1980**, *102*, 7816–7817.
- [26] A. D. de Araújo, J. M. Palomo, J. Cramer, M. Köhn, H. Schröder, R. Wacker, C. Niemeyer, K. Alexandrov, H. Waldmann, *Angew. Chem.* **2006**, *118*, 302–307; *Angew. Chem. Int. Ed.* **2006**, *45*, 296–301.
- [27] K. W. Hill, J. Taunton-Rigby, J. D. Carter, E. Kropp, K. Vagle, W. Pieken, D. P. C. McGee, G. M. Husar, M. Leuck, D. J. Anziano, D. P. Sebesta, *J. Org. Chem.* **2001**, *66*, 5352–5358.
- [28] T. M. Tarasow, S. L. Tarasow, B. E. Eaton, *Nature* **1997**, *389*, 54–57.
- [29] M. N. Yousaf, M. Mrksich, *J. Am. Chem. Soc.* **1999**, *121*, 4286–4287.
- [30] R. Tona, R. Häner, *Bioconjugate Chem.* **2005**, *16*, 837–842.
- [31] D. J. Slamon et al., *Science* **1989**, *244*, 707–712 (see the Supporting Information for the complete reference).
- [32] S. M. Chamow, T. P. Kogan, D. H. Peers, R. C. Hastings, R. A. Byrn, A. Ashkenazi, *J. Biol. Chem.* **1992**, *267*, 15916–15922.
- [33] G. T. Hermanson, *Bioconjugate techniques*, Academic Press, San Diego, CA, **1996**, pp. 456–493.